Supporting Information

Tracking the optical mass centroid of single electroactive nanoparticles reveals electrochemically inactive zone

Wenxuan Jiang, Wei Wei, Tinglian Yuan, Shasha Liu, Ben Niu, Hui Wang* and Wei Wang*

State Key Laboratory of Analytical Chemistry for Life Science, School of Chemistry and Chemical Engineering, Nanjing University, Nanjing 210023, China

*Corresponding authors

Table of Contents

S1. Characterization of as-synthesized PB nanoparticles

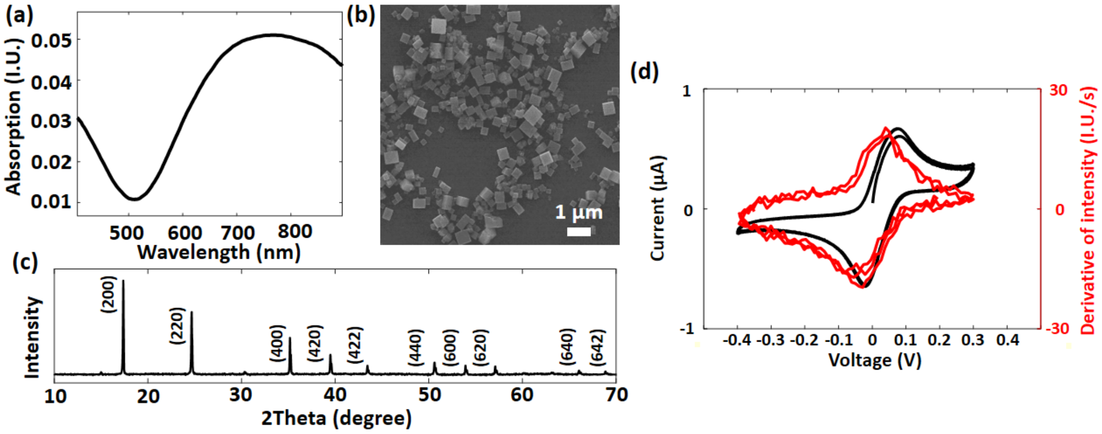

Figure S1. (a) The UV-vis spectrum of as-synthesized PB nanoparticle aqueous solution. (b) The SEM image of as-synthesized PB nanoparticles deposited on ITO surface. (c) The XRD pattern of PB nanoparticles and the crystallite size can be estimated by the Scherrer equation: $D_{hkl} = K\lambda/(B_{hkl}\cos\theta)$, where D_{hkl} is the crystallite size in the direction perpendicular to the lattice planes, *hkl* are the Miller indices of the lattice planes being analyzed, K is a numerical factor frequently referred to as the crystallite-shape factor (Scherrer constant, 0.89), λ is the wavelength of X-rays, B_{hkl} is the full-width at half-maximum of the X-ray diffraction peak in radians and θ is the Bragg angle. (d) Bulk current as a function of potential (black curve). The first-order derivative of scattering intensity curve for an individual PB nanoparticle during redox reaction (red curve).

S2. Materials and Methods

Synthesis and characterizations of PB nanoparticles

The PB nanoparticles were synthesized in the light of previous mature protocol reported in the literature[1]. 100 mL hydrochloric acid aqueous solution was mixed with 422 mg $K_4Fe(CN)_6 \cdot 3H_2O$ powder to form the initial reactant with the concentration of 0.1 mol/L. After immerging into an ultrasonic bath at 36 °C for 80 minutes, the product was centrifuged at 14800 rpm for 20 minutes to collect PBNPs. The obtained sample was washed with deionized water (DIW, 18 MΩ·cm, Milli-Q, Smart2Pure 3 UF, Thermo Fisher) three times and dried in the vacuum oven at 25 °C for 12 hours, and the PBNPs sample was ready for the experiment.

The morphology and interior structure of PBNPs were characterized by the scanning electron microscope (JEOL, JSM-7800F). The UV-vis spectrum of aqueous solution containing PBNPs was collected by a Cary series UV-vis spectrophotometer (Agilent Technologies). The X-ray diffraction (XRD) pattern was captured by a Bruker AXS D8 ADVANCE instrument applying Cu Kα radiation at 40 kV and 40 mA.

Preparation of the electrochemical cell and electrodes

The ITO-coated glass slides with the thickness of 1.1 mm (8 ohms/square) were obtained from Wuhan Jinge-Solar Energy Technology Co. Ltd.. Each slide was cleaned in an ultrasonic bath for 30 minutes by immersing into acetone, ethanol and DIW, respectively. After drying with nitrogen gas, 100 μL droplet of 200-fold diluted PBNP solution was added to the cleaned ITO-coated slide and dried under vacuum (3 hours) for depositing PBNPs on the surface. The slide deposited with individual PBNPs was washed with DIW, and dried with nitrogen gas. A polydimethylsiloxane (PDMS) cell was placed in the top of ITO slide coated with PB nanoparticles, and another clean ITO slide was placed to cover the upper surface of PDMS cell for building the two-electrode system of the electrochemical cell as shown in Fig S1. Two Cu wires were sticked to the top and bottom ITO slides for building the connection with external electrochemical setup. 0.1 M KNO_3 electrolyte solution was performed a deoxygenation operation before electrochemical measurement to remove oxygen reduction reaction.

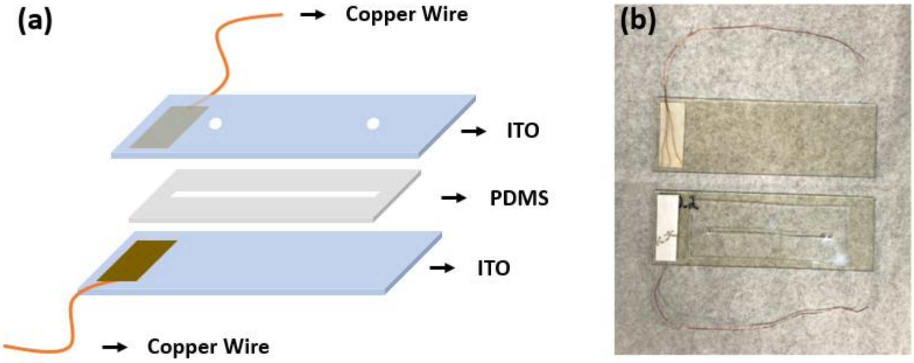

Figure S2. (a) Schematic illustration of electrochemical system. (b) Physical diagrams of electrochemical system.

Optical imaging and electrochemical measurement

The optical images of single PBNPs were captured by an inverted dark-field microscope (Eclipse Ti-U, Nikon), which was equipped with an oil-immersed dark-field condenser (NA=1.20-1.43), a water-immersed objective lens (NA=1.0, 60×, part number MRF07620), and a quartz tungsten halogen lamp (LV-LH50PC, Nikon) worked as the light source. The color optical images were captured by the DS-Ri2 camera (Nikon), and the monochrome images were collected from a charged coupled device (CCD, Pike F032B, Allied Vision Technologies). The dark-field scattering spectrums were measured by a grating spectrometer (Acton Spectra Pro SP-2300, Princeton Instruments).

All the electrochemical experiments were performed with a potentiostat (Autolab PGSTAT302N, Metrohm AG), which was modulated via an external waveform function generator (Agilent, 33220A). The voltage of triangular and square waves was applied to the two-electrode system with the same parameters (t=120 s, V_{pp}=0.6 V, Offset=0 V). As shown in Fig S2, scattering intensity of PBNPs tends to be stable and the reaction reaches equilibrium when the applied potential is greater than 0.3 V or less than -0.3 V which is the reason why we selected electrochemical window between -0.3 V ~ +0.3 V. A data acquisition board (DAQ, USB- 6281, National Instruments) was introduced to synchronize the electrochemical signals from potentiostat and optical signal from the camera. By sweeping the cyclic voltage to acquire AC modulation, the dark-field scattering images of single PB nanoparticles were collected directly by the color camera, or captured by the CCD camera after passing through a 700 nm long-pass filter (FELH0700, Thorlabs).

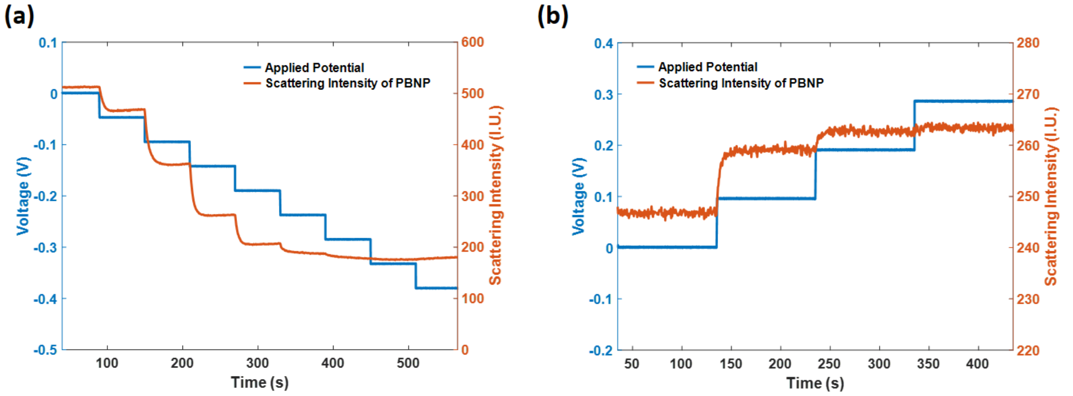

Figure S3. (a) Scattering intensity of PBNPs when applying a reduced step potential. (b) Scattering intensity of PBNPs when applying an oxidation step potential.

Data analysis for extracting OMC

For tracking the OMC of single PB nanoparticle accurately during electrochemical reaction, the two-dimensional (2-D) Gaussian fitting with a least-squares-based library function (lsqcurvefit) in MATLAB was introduced. The dark-field scattering pattern of individual PBNP can be fitted by the equation:

$$I(x,y) = B + I_0 exp\left[-\frac{1}{2}\left[\left(\frac{x - x_0}{\sigma_x}\right)^2 + \left(\frac{y - y_0}{\sigma_y}\right)^2\right]\right]$$

where $I(x,y)$ is the dark-field scattering intensity of a diffraction-limited pattern of single PB nanoparticle, B is the optical intensity of background without nanoparticles, I_0 is the intensity of 2-D Gaussian fitting, x_0 and y_0 are the initial coordinates of the OMC, x and y are the varied coordinates of the OMC during electrochemical reaction, and σ_x and σ_y are the standard deviation in x and y, respectively.

S3. Determination of scattering intensity and equivalent radius for individual PBNPs in Figure 1f

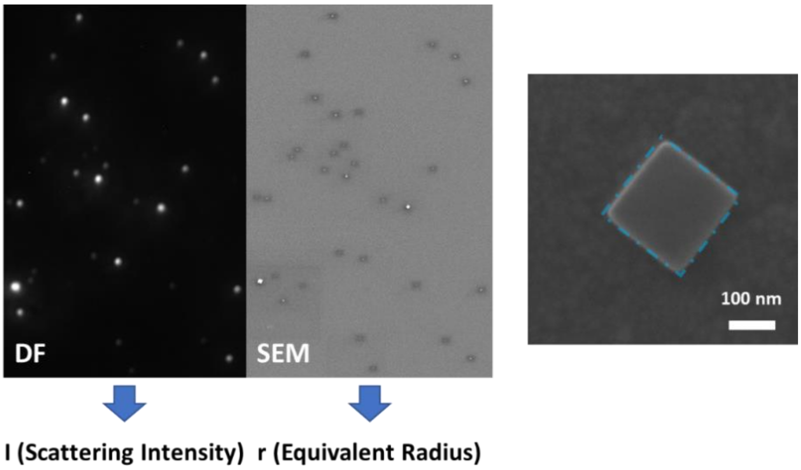

Figure S4. Determination of scattering intensity extracted from dark-field image, and equivalent radius (r) obtained for single PBNPs from SEM image according to the equation: $\mathrm{r} = \sqrt{S/\pi}$.

S4. Drift correction of OMC shift

Polystyrene nanoparticles (PSNPs) with a diameter of 500 nm were added to the system and attached to the substrate for drift correction. As shown in Fig S3, sample drift of the system was calculated by fitting the point spread function of those PSNPs with a 2D Gaussian because PSNPs had no electrochemical response during our experiments. Every OMC result shown in the manuscript had been already corrected by subtracting the OMC change of PSNPs.

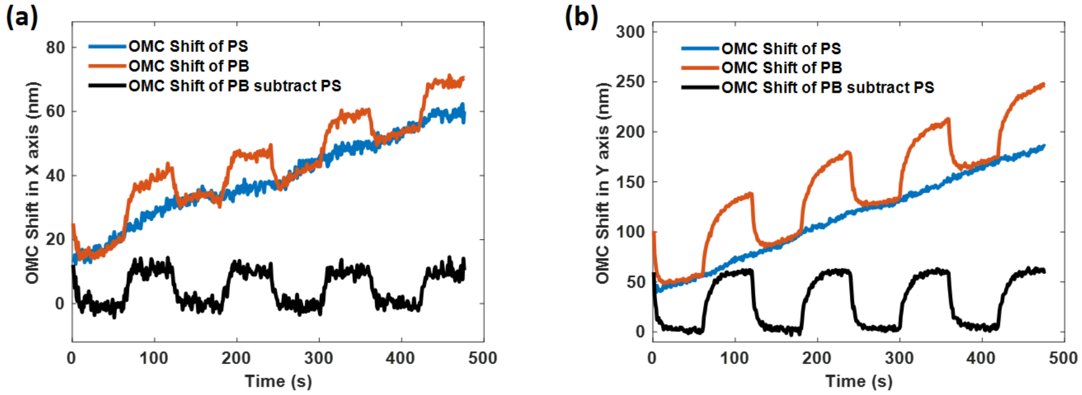

Figure S5. (a) OMC shift of PSNP and PBNP in X axis. (b) OMC shift of PSNP and PBNP in Y axis.

S5. Statistical analysis of OMC displacement between PB and PW state for individual entities

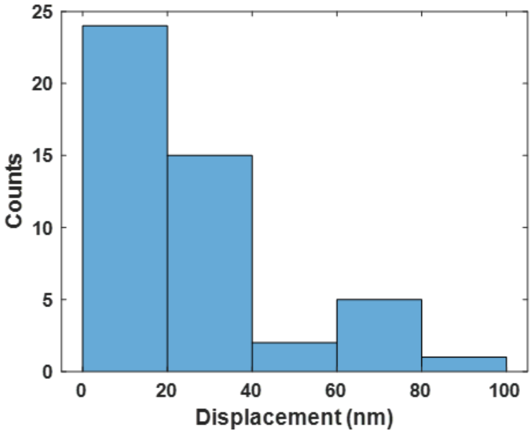

Figure S6. Statistical analysis of the OMC displacement between PB and PW state for 47 entities.

S6. Reversible trajectory of OMC for single PBNP

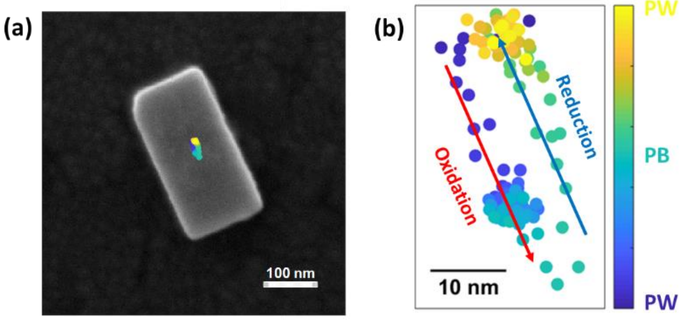

Figure S7. (a) The SEM image of single PB nanoparticle and trajectory of OMC. (b) The trajectory of the optical mass centroid for the PBNP in a during one cycle of electrochemical redox reaction.

S7. Corresponding current curve and voltage curve for the cycling in manuscript

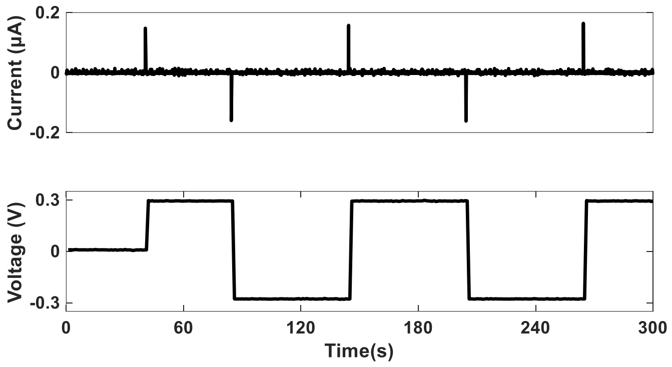

Figure S8. The corresponding current curve and voltage curve for the cycling in Figs. 1b-c and Fig. 2a.

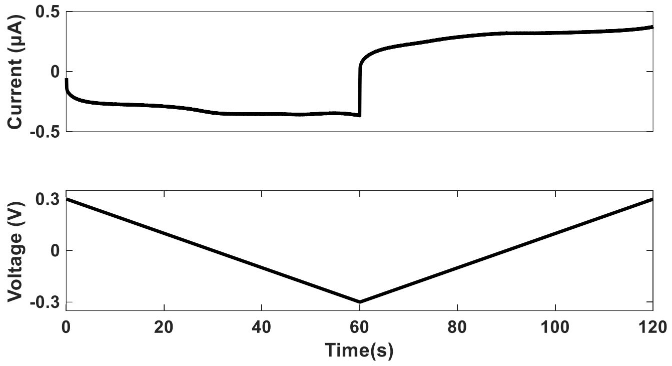

Figure S9. The corresponding current curve and voltage curve for the cycling in Fig. 2b.

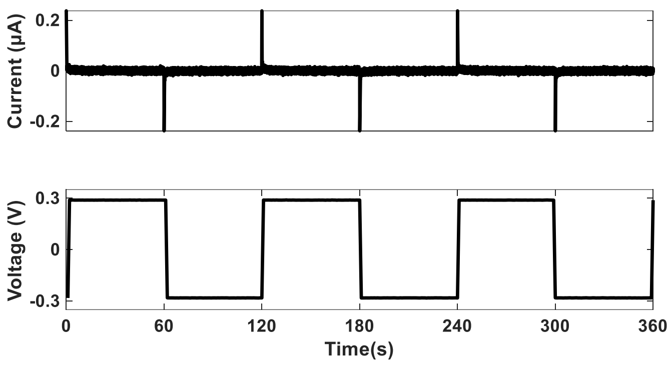

Figure S10. The corresponding current curve and voltage curve for the cycling in Fig. 3.

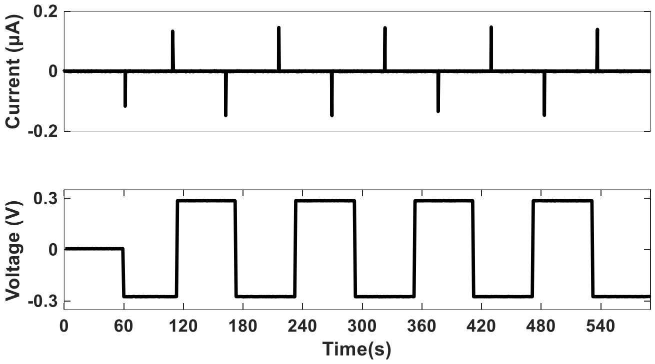

Figure S11. The corresponding current curve and voltage curve for the cycling in Fig. 6.

S8. Description of Movies

Movie S1. Dark-field imaging of individual PB nanoparticles captured by DS-Ri2 camera during applying cyclic square-wave voltage from +0.3 V to -0.3 V in **Figures 1b-c and Figure 2a**.

Movie S2. Dark-field imaging of individual PB nanoparticles captured by CCD camera during applying cyclic square-wave voltage from +0.3 V to -0.3 V in **Figure 3a**. The scattering intensity of most nanoparticles varies with voltage, and that of the remaining particles show no obvious variation attributed to electrochemical inactivity.

Movie S3. Dark-field imaging of a PB nanoparticle during cycling square-wave voltage, and the synchronous trajectory of OMC (**Figure 6**).

Reference

1. X. L. Wu, M. H. Cao, C. W. Hu and X. Y. He, *Crystal Growth & Design*, 2006, **6**, 26-28.